Solvation of benzene derivatives in SC-CO_2: a molecular dynamics study of fluorination effects†

Nicolas Galand and Georges Wipff*

Institut de Chimie, 4 rue B. Pascal, 67 000, Strasbourg, France.
E-mail: wipff@chimie.u-strasbg.fr

Received (in Montpellier, France) 17th April 2003, Accepted 16th June 2003
First published as an Advance Article on the web 12th August 2003

According to a molecular dynamics study of benzene (C_6H_6) and its derivatives C_6F_6, CH_3–C_6H_5 and CF_3–C_6H_5 in SC-CO_2 solution, the fluoro compounds are better solvated than the H analogs. This is supported by the analysis of average solute-solvent interaction energies and by free energy perturbation simulations at 305 and 350 K. Stepwise model building of $C_6X_6(CO_2)_n$ aggregates (X = H and F) in the gas phase, however, indicates that up to $n = 6$, interactions with CO_2 are stronger with benzene, while perfluorobenzene becomes better solvated at higher coordination numbers. Thus, the enhancement of the CO_2-philicity upon fluorination does not stem from enhanced individual interactions with the CO_2 molecule, but from the higher coordination number, due to the increase of solvent accessible surface. Finally, simulations of C_6H_6 and C_6F_6 at the CO_2–water interface reveal that the former is somewhat surface active due to specific O–H$\cdots\pi$ facial interactions between interfacial water molecules, while C_6F_6 mostly sits in the CO_2 phase, in keeping with its larger CO_2-philicity.

Introduction

It is generally considered that the H → F substitution in alkyl or aromatic compounds enhances their solubility in supercritical CO_2 (SC-CO_2),[1–5] but the reasons of this enhanced CO_2-philicity remains unclear. Whether this is due to specific interactions remains controversial.[6,7] For instance, IR spectrocopic studies on butanol *vs.* perfluorobutanol did not reveal specific interactions.[8] A similar conclusion was obtained from an NMR study of perfluorobenzene *vs.* benzene[9] while another NMR study of *n*-hexane *vs.* perfluorohexane concluded that specific interactions between CO_2 and fluorine existed.[10] Similar controversies arose from theoretical approaches, like quantum mechanical studies on CO_2 clusters around ethane *vs.* perfluoroethane.[11–13] Interactions are weak and the results are quite sensitive to the level of theory and basis set used for these simulations.[6] So far, to our knowledge, no convincing explanation has emerged from the study of dimers or small aggregates in the gas phase concerning the enhanced CO_2-philicity upon fluorination. Solvation is a complex process that results from the interplay between solute-solvent and solvent-solvent interactions, involving enthalpic and entropic contributions.

This led us to simulate the solution behavior of simple compounds, thus accounting for their temperature-dependent dynamics features. Following our first simulations on SC-CO_2 solutions and aqueous interfaces,[14] we decided to compare simple aromatics and their fluoro analogs in SC-CO_2 using molecular dynamics (MD) simulations based on standard CO_2 potentials. More specifically, we have focussed on aromatic solutes (hereafter noted Aryl): benzene *vs.* perfluorobenzene and toluene *vs.* trifluoromethyltoluene. They will be denoted in short as X-Benz or X-Tol (with X = F and H; see Fig. 1). Our aim is to compare the solvation of these compounds in CO_2: characteristics of the first solvation shell (radius, coordination number CN, lifetime, interaction energy with CO_2) and differences in Gibbs free energies of solvation. We also analyze their stepwise solvation by comparing the Aryl(CO_2) dimers (Aryl = X-Benz and X-Tol) and X-Benz-$(CO_2)_n$ aggregates in the gas phase. Finally, the aryl molecules will be simulated at an aqueous interface with CO_2 in order to compare their interfacial activity. In contrast to many fluorinated compounds that are used, for example in liquid-liquid assisted ion extraction,[1,15,16] they lack an amphiphilic topology, but it will be shown that they behave differently, upon H/F substitution.

Methods

Empirical representation of the potential energy

The simulations were performed with the modified AMBER5.0 software[17] in which the potential energy is described by the sum of bond, angle and dihedral deformation

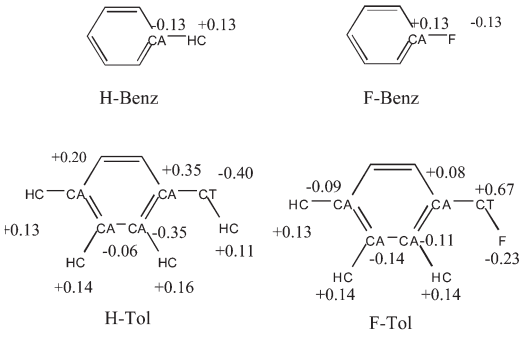

Fig. 1 Simulated X-Aryl molecules (C_6H_6, C_6F_6, C_6H_5–CH_3 and C_6H_5–CF_3) with their acronyms, AMBER types and atomic charges.

† Electronic supplementary information (ESI) available: structures and interaction energies of X-Benz$(CO_2)_n$ aggregates in the gas phase and table of force field parameters. See http://www.rsc.org/suppdata/nj/b3/b304300b/

energies, and pairwise additive 1–6–12 (electrostatic + van der Waals) interactions between non-bonded atoms.

$$U = \Sigma_{\text{bonds}} K_r (r - r_{\text{eq}})^2 + \Sigma_{\text{angles}} K_\theta (\theta - \theta_{\text{eq}})^2 + \Sigma_{\text{dihedrals}} \Sigma_n V_n (1 + \cos n\varphi) + \Sigma_{i<j} [q_i q_j / R_{ij} - 2\varepsilon_{ij} (R_{ij}^*/R_{ij})^6 + \varepsilon_{ij} (R_{ij}^*/R_{ij})^{12}]$$

The aryl charges were derived from ESP potentials calculated with the 6-31G* basis set. They are given with the AMBER atom types in Fig. 1 and the list of force field parameters is given in Table S1 (Electronic supplementary information, ESI). The fluorine non-bonded parameters ($R^*_F = 1.75$ Å, $\varepsilon_F = 0.061$ kcal mol^{-1}) were those of Kollman *et al.*.[18] The solvent models were derived from studies on the liquid properties. CO_2 was represented by the three-points model of Murthy *et al.*[19] (charges $q_C = 0.596$, $q_O = -0.298$ e and van der Waals parameters $R^*_O = 1.692$, $R^*_C = 1.563$ Å and $\varepsilon_O = 0.165$, $\varepsilon_C = 0.058$ kcal mol^{-1}) and water was represented with the TIP3P model.[20] All O–H, C–H bonds and the C=O bonds of CO_2 were constrained with SHAKE, using a time step of 2 fs. The intramolecular electrostatic and van der Waals 1–4 interactions were scaled down by a factor 2.0. Non-bonded interactions were calculated with an atom-based cutoff of 12 Å for all systems, in conjunction with a reaction field (RF) correction to the Coulombic interactions.[21] This model assumes that the charge distribution within a sphere of cutoff radius interacts with a polarizable dielectric medium and prevents discontinuities of the potential energy at the cutoff boundaries. Such a cutoff is sufficient, given the dominant short-range character of the interactions in such systems.[22] The non-bonded pair lists were updated every ten steps.

Solutions and dynamics

An aryl molecule was immersed in a cubic CO_2 box of ≈30–35 Å length, containing ≈350–400 CO_2 molecules (Fig. 2). The corresponding density is 0.80 g cm^{-3}, which is above the critical density (0.47 g cm^{-3} at 304 K) and close to the experimental density of 0.79 g cm^{-3} at 345 K and a pressure of 30 MPa.[23] The solutions were represented with 3D periodic boundary conditions. The CO_2–water interface has been built as indicated in references 14 and 24, starting with adjacent boxes of CO_2 and pure water. The characteristics of the simulated solutions are given in Table 1.

After energy minimization, MD in solution was run at 350 or 305 K and constant volume, first for 50 ps with the solute frozen (in order to relax the solvent molecules), followed by free MD. The temperature was monitored by separately coupling the solvent(s) and solute subsystems to thermal baths at the reference temperature with a relaxation time of 0.2 ps for the solvents and 0.5 ps for the solutes, using the Berendsen algorithm.[25] MD in the gas phase on Aryl(CO_2) dimers and Aryl(CO_2)$_n$ aggregates was run at a low temperature (10 or 30 K) in order to prevent dissociation.

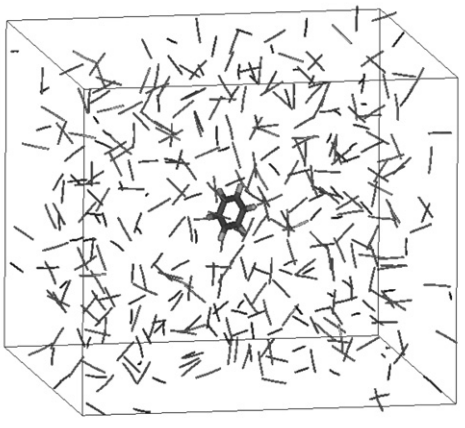

Fig. 2 : The simulation CO_2 box with one aryl solute.

Table 1 Characteristics of the simulated solutions

Solute	T/K	Box size/Å^3	N_{CO2}/N_{H2O}	Time/ns
H-Benz	350	34 × 35 × 29	394/0	0.6
F-Benz	350	34 × 35 × 29	402/0	0.6
H-Tol	350	29 × 32 × 33	333/0	0.6
F-Tol	350	30 × 32 × 33	346/0	0.6
H-Benz	305	34 × 35 × 29	394/0	0.6
F-Benz	305	34 × 35 × 29	402/0	0.6
H-Benz	350	26 × 27 × (30 + 32)	245/735	1.0
F-Benz	350	27 × 27 × (30 + 32)	249/740	1.0
H-Benz	305	36 × 36 × (35 + 35)	500/1500	0.5
F-Benz	305	36 × 36 × (35 + 29)	500/1200	0.5

Free energy calculations

The difference in free energies of hydration between H/F compounds was obtained using the statistical perturbation FEP theory and the windowing technique,[26] with

$$\Delta G = \sum \Delta G_\lambda \quad \text{and} \quad \Delta G_\lambda = RT \text{Log} \left\langle \exp \frac{(U_\lambda - U_{\lambda+\Delta\lambda})}{RT} \right\rangle_\lambda$$

The potential energy U_λ was calculated using a linear combination of mutated parameters of the initial state ($\lambda = 1$) and final state ($\lambda = 0$): $A_\lambda = \lambda \cdot A_1 + (1 - \lambda) \cdot A_0$. The mutated parameters involve non-bonded ones (atomic charges and van der Waals R^* and ε), as well as the bonded parameters (K_r and r_{eq} for the bonds, K_θ and θ_{eq} for the angles; dihedral contributions remained the same). The number of intermediate steps (''windows'') was 21. At each window, 2 ps of equilibration was followed by 3 ps of data collection and the change of free energy ΔG_λ was averaged from the forward and backward cumulated values.

Analysis of results

The results have been analyzed as described from the trajectories saved every 0.5 ps. The energy component analysis of the trajectories was performed in terms of pairwise additive contributions (electrostatic, van der Waals and total) of the solvent and the solute. The distribution of CO_2 molecules was characterized by their radial distribution functions (RDFs) around the center-of-mass of the aryl ring.

Results

We first analyze the interactions of a H/F-Aryl molecule with a single CO_2 molecule and the stepwise formation of X-Benz-(CO_2)$_n$ aggregates in the gas phase. This is followed by the analysis of the solvation properties of H/F-Aryl in bulk CO_2 solution and a comparison at the CO_2–water interface.

Interactions between a single CO_2 molecule and H/F-aryls in the gas phase

Several arrangements of Aryl(CO_2) ''complexes'' were initially considered, in order to compare the facial *vs.* in-plane coordination of CO_2, and the preferred orientations of CO_2. The four aromatics studied display stronger interactions with facial CO_2, but the preferred structure depends on their F/H substituents (see Fig. 3).

In the H-Benz(CO_2) dimer, CO_2 sits parallel to the aryl ring with its C atom close to the center. This agrees with

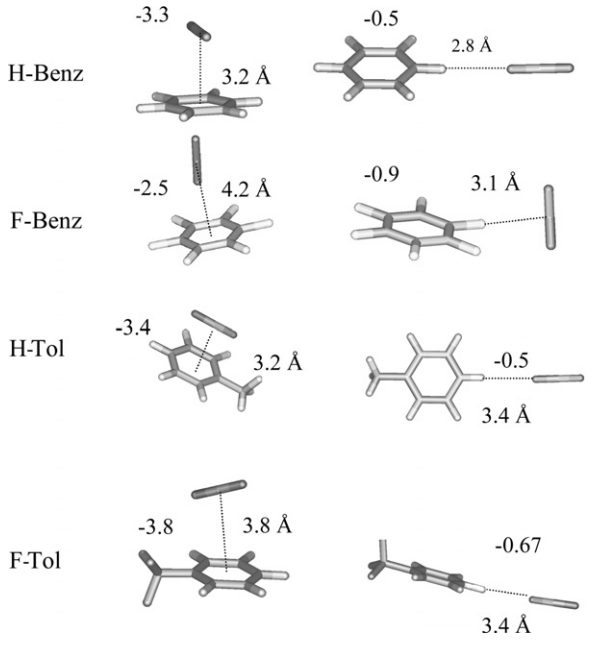

Fig. 3 Most stable X-Benz(CO_2) and X-Tol(CO_2) dimers in the gas phase after 1 ns of dynamics at 10 K. Interaction energies (kcal mol^{-1}) for facial (left) and in-plane "complexes" (right). See text.

spectroscopic[27] and other computational studies.[28] During the dynamics at 10 K, the CO_2 molecule is immobile but at 30 K, it rotates "clockwise" on the π-face of H-Benz (Fig. 4). This structure contrasts with the corresponding F-Benz(CO_2) "complex" in which CO_2 is "perpendicular" to the ring and displays during the dynamics at 30 K a "precessional" motion around the C_6 symmetry axis (Fig. 4). Coordination patterns follow the quadrupole-quadrupole interactions between X-Benz and CO_2 and the quadrupole inversion upon H → F substitution of the aromatic ring. Note that the interaction energy with CO_2 is somewhat more attractive with H-Benz than with F-Benz (−3.1 and −2.6 kcal mol^{-1}, respectively). As electrostatic interactions are comparable in both complexes (−1.1 and −1.2 kcal mol^{-1}), the preference for H-Benz mostly stems from more favorable van der Waals contacts.

In the H-Tol and F-Tol "complexes", the CO_2 molecule lies parallel to the ring. It interacts somewhat better than with benzene (by 0.3 and 0.1 kcal mol^{-1}, respectively) due to secondary van der Waals attractions with the CH_3 or CF_3 groups.

In-plane coordination of CO_2 is less stable and led, upon optimization, to the facial complexes described above. This is why in-plane coordination was investigated by constraining the C_{Aryl}–X–C_{CO2} angle to 180° and letting the CO_2 molecule relax during a MD simulation of 1 ns at 10 K. The potential energy displays quite shallow minima and the best arrangement is determined by the electrostatics. H-Benz, H-Tol and

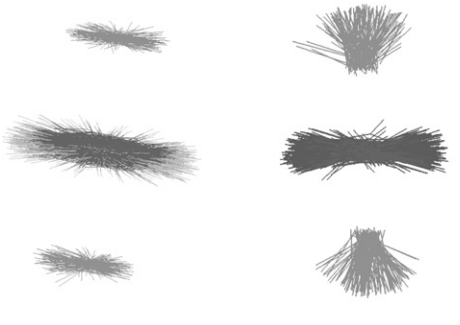

Fig. 4 : H-Benz(CO_2)$_2$ (left) and F-Benz(CO_2)$_2$ "complexes" (right) simulated *in vacuo* at 30 K: cumulated views over 100 ps.

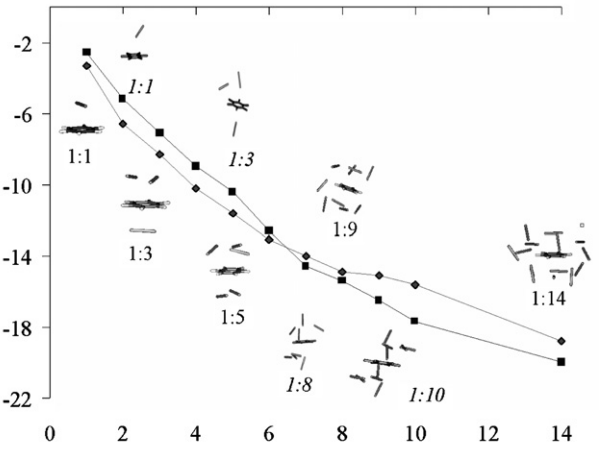

Fig. 5 The X-Benz(CO_2)$_n$ aggregates in the gas phase: average interaction energies (kcal mol^{-1}) between X-Benz and CO_2 as a function of n for the most stable arrangements. Averages are over 200 ps. Diamonds (◆) for H-Benz and squares (■) for F-Benz.

F-Tol prefer a "linear" C–H···O=C coordination (at 2.8, 3.4 and 3.4 Å, respectively) while F-Benz prefers to have CO_2 perpendicular to the C–F bond and to the ring. This allows for primary C–F···CO_2 attractions while minimizing the repulsions between *ortho* F atoms of F-Benz and O_{CO_2} atoms. The stabilization energies for in-plane dimers range from −0.4 to −0.9 kcal mol^{-1}, which is less than for facial dimers. Comparing the in-plane F-Benz *vs.* H-Benz adducts with CO_2, we notice that the former is preferred (by ≈0.5 kcal mol^{-1}) while facial coordination favors H-Benz, also by ≈0.5 kcal mol^{-1}. It can thus be anticipated that further coordination of CO_2 molecules will be facial and generally more favorable with the H-Aryls than with the F-Aryls. This is indeed observed in the first X-Benz aggregates in which CO_2 was added stepwise.

Stepwise formation of CO_2 aggregates with H-benzene *vs.* F-benzene in the gas phase

In this section, we consider H/F-Benz(CO_2)$_n$ aggregates, with $n = 2$ to 14. For the smaller ones ($n < 6$), we compare different arrangements ($n = p + q$) with p and q molecules on each face of the ring. The results [Figs. 5, Fig. S1 (ESI) and Table 2] show that the CO_2 molecules first cover the two faces of the ring. For the trimer ($n = 2$), the 1 + 1 facial complexes of H-Benz and F-Benz are more stable than the 2 + 0 complexes in which the CO_2···CO_2 interactions are somewhat repulsive. Similarly for $n = 3$, both 2 + 1 complexes are more stable than the 3 + 0 complexes (by ≈0.6 kcal mol^{-1}) and, for $n = 4$, 2 + 2 complexes are preferred over 1 + 3 ones (by ≈0.5 kcal mol^{-1}). The important result, as far as the fluoro effect is concerned, is the smaller interaction energy of F-Benz with CO_2, compared

Table 2 X-Benz(CO_2)$_n$ aggregates in the gas phase: average CO_2/X-Benz interaction energies (kcal mol^{-1}) for different arrangements. See snapshots in Figure S1.

n	Arrangement	H-Benz	F-Benz
1	(1 + 0)	−3.3	−2.6
2	(1 + 1)	−6.6	−5.2
2	(2 + 0)	−5.0	−5.0
3	(2 + 1)	−8.3	−7.1
3	(3 + 0)	−7.6	−6.6
4	(3 + 1)	−9.7	−8.6
4	(2 + 2)	−10.2	−9.0
5	(3 + 2)	−11.6	−10.5

Table 3 X-Aryls in a SC-CO_2 solution at 305 and 350 K. Characteristics of the first solvation shell: radius R (Å), average coordination number (CN), average X-Aryl/CO_2 interaction energies (electrostatic, van der Waals and total, in kcal mol^{-1}). ΔE is the total interaction energy with the CO_2 liquid.

Solute	T	R	CN	Elect	vdW	Total	ΔE
H-Benz	350	7.0	13.0 ± 2.4	0.9 ± 0.9	-7.5 ± 1.5	$-8.4. \pm 1.8$	-9.0 ± 1.8
F-Benz	350	7.7	18.2 ± 2.4	-1.3 ± 1.0	-8.7 ± 1.9	-11.0 ± 1.9	-11.5 ± 1.9
H-Tol	350	7.2	14.4 ± 1.9	-0.7 ± 0.8	-8.5 ± 1.4	-9.2 ± 1.7	-9.8 ± 1.6
F-Tol	350	7.8	20.6 ± 1.06	-1.0 ± 0.9	-9.0 ± 1.2	-10.0 ± 2.0	-10.5 ± 2.0
H-Benz	305	7.0	13.1 ± 2.4	-1.5 ± 0.9	-8.5 ± 1.3	-10.0 ± 1.8	-10.3 ± 1.6
F-Benz	305	7.7	19.8 ± 2.4	-1.5 ± 0.9	-10.4 ± 1.6	-11.9 ± 1.9	-12.5 ± 1.9

to H-Benz (by 1.4, 1.2, and 0.5 kcal mol^{-1}, for $n = 2$, 4, 6). However, in larger aggregates ($n > 6$), the preference inverts in favor of F-Benz. There are several reasons for this. (i) First, steric hindrance prevents optimal coordination of several facial CO_2 molecules and steric hindrance is more important when CO_2 is parallel, instead of perpendicular to the ring, thus penalizing H-Benz more than F-Benz. (ii) Second, as the first solvation shell builds up, some CO_2 molecules come closer to the ring plane, thus favoring the F-Benz solute. (iii) Finally, F-Benz has a larger solvent accessible surface than H-Benz (112 *vs* 66 Å^2) and can therefore accommodate a larger number of solvent molecules in its first solvation shell.

Solvation of X-Aryls in CO_2 solution. Structural and energetic features

Extrapolation of the trends observed in Aryl$(CO_2)_n$ clusters to a bulk liquid solution is expected to lead to preferential solvation of the F-Aryls. It should be pointed out, however, that gas phase clusters were studied at low temperatures (10 or 30 K), allowing for tight Aryl···CO_2 contacts, while in the supercritical solution the CO_2 molecules diffuse rapidly and their lifetime in the first coordination shell is small, leading to non-optimal interactions with the solutes. This will be analyzed below. The important result, in the context of F/H substitution, is the better solvation of the F-Aryl compounds in SC-CO_2 solution.

The analysis of Aryl···solvent interaction energies (ΔE) at 350 K (see Table 3) indeed show that ΔE is larger (more negative) with F-Benz than with H-Benz (-11.5 ± 2.1 *vs.* -9.0 ± 1.8 kcal mol^{-1}) and larger with F-Tol than H-Tol (-10.5 ± 2.0 *vs.* -9.8 ± 1.7 kcal mol^{-1}). Notice the high fluctuations in the ΔE values (about 2 kcal mol^{-1}), in keeping with the versatile coordination modes and rapid diffusion of CO_2 molecules. As expected, ΔE is mainly due to the van der Waals energy component, while the electrostatic component, although attractive, is small (< 1 kcal mol^{-1}). Thus, the preference for F- *vs* H-Aryls stems from the van der Waals contribution. The latter also favors toluene, compared to benzene (by $\approx$1 kcal mol^{-1}). The effect of temperature has been investigated for the H/F-Benz solutions and a decrease from 350 K to 305 K is found to increase the magnitude of ΔE (by $\approx$1 kcal mol^{-1}). The difference between H-Benz and F-Benz is retained ($\approx$2 kcal mol^{-1}), however. We notice that these ΔE are $\approx$0.5–2 kcal mol^{-11} smaller than the interaction energies between these solutes and an aqueous medium (for example the interaction energies of H-Tol and F-Tol with a pure TIP3P water solution are respectively -12.2 and -13.7 kcal mol^{-1}). Thus, the higher solubility of these hydrophobic solutes in CO_2, compared to water, cannot simply be explained on the basis of solute···solvent interactions only, but depends on other factors as well (*e.g.*, solvent reorganization and cavitation energies).[29]

A more dramatic temperature effect is seen when H-Benz and F-Benz are simulated in the CO_2 "solution" for 1 ns at 10 K without periodic boundary conditions. This does not correspond to supercritical conditions anymore, but to an energy minimized "supercluster" in the gas phase. The solute-"solvent" interactions (-22.5 ± 0.3 kcal mol^{-1} for H-Benz and -28.4 ± 0.2 kcal mol^{-1} for F-Benz) increase by more than 10 kcal mol^{-1}, compared to the solution at 350 K, thus demonstrating the importance of dynamics and lifetime of the solute-solvent interactions. At 10 K however, the perfluorobenzene molecule interacts better than benzene with CO_2 (by $\approx$6 kcal mol^{-1}) and the difference is magnified by more than 3, when compared to the supercritical conditions.

In principle, free energy calculations account for the enthalpic and entropic changes upon H $\rightarrow$ F mutations and the results (Table 4) confirm that fluoro compounds are better solvated that their hydrogenated analogs. At 350 K, the corresponding $\Delta G_{F/H}$ amounts to -0.7 ± 0.03 kcal mol^{-1} for the H-Tol to F-Tol mutation and to -1.4 ± 0.02 kcal mol^{-1} for the H-Benz to F-Benz mutation, thus following the trends in ΔE noted above. Repeating the H-Benz to F-Benz mutation at 305 K somewhat enhances the preference for F-Benz ($\Delta G_{F/H} = -1.6 \pm 0.02$ kcal mol^{-1}). This is consistent with somewhat tighter contacts with the solvent at the lower temperature, therefore enhancing van der Waals interactions.

Table 4 : Changes in free energy (kcal mol^{-1}) upon H-to-F mutations in CO_2 solution.

Mutation	T/K	ΔG "forward"	ΔG "backward"	$\Delta G_{H/F}$
H-Tol $\rightarrow$ F-Tol	350	-0.69	-0.74	-0.7
H-Benz $\rightarrow$ F-Benz	350	-1.42	-1.44	-1.4
H-Benz $\rightarrow$ F-Benz	305	-1.59	-1.64	-1.6
H-Benz $\rightarrow$ F-Benz	60	-3.86	-3.93	-3.9

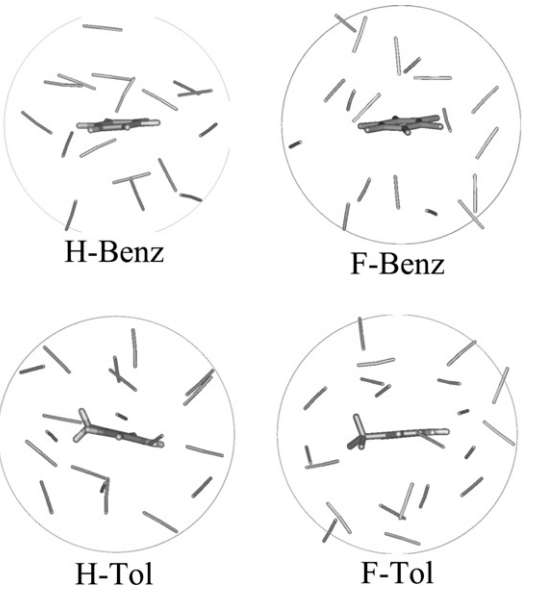

Fig. 6 X-Benz and X-Tol (X = H, F) in CO_2 solution at 350 K: snapshots of the first solvation shell.

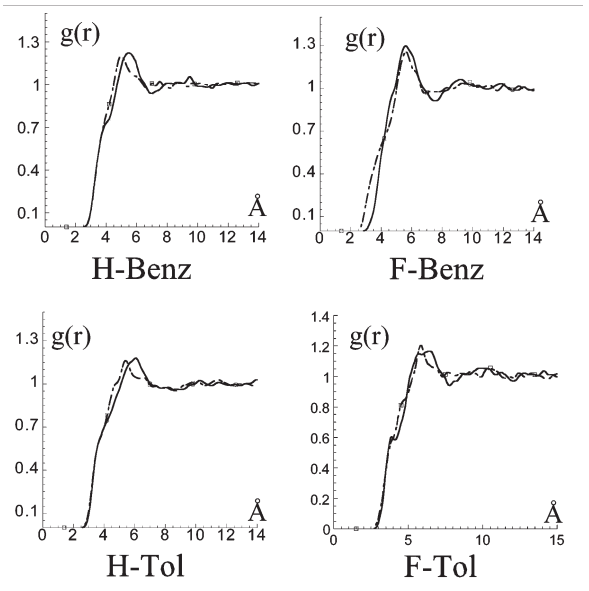

Fig. 7 X-Benz and X-Tol (X = H, F) in SC-CO_2 solution at 350K: RDF g(r) of O_{CO_2}(dotted line) and C_{CO_2} (full line) around the center of the ring as a function of the distance (Å). Averages over the last 0.2 ns.

We thus attempted to simulate this mutation at 10 or 20 K for 1 ns, but the sampling was not sufficient due to the too low kinetic energy. At 60 K, however, we calculated a $\Delta G_{F/H}$ value of -3.9 kcal mol^{-1}, thus confirming the effect of temperature and dynamics on the fluoro effect.

The analysis of the solvent characteristics around the solutes reveals interesting features. The arrangement of first-shell CO_2 molecules (see Fig. 6) is reminiscent of what was observed in the gas phase clusters. In particular, on the faces of the ring, CO_2 is rather parallel to H-Benz, H-Tol and F-Tol and perpendicular to F-Benz. We now discuss in more detail H-Benz *vs.* F-Benz, which display the largest change in solvation energies and are simple to analyze, due to their higher symmetry. Typical solvent RDFs around their center-of-mass are shown in Fig. 7. Around both solutes, the RDFs display a first broad peak at ≈6 Å, followed by a shallow minimum (for H-Benz) or a plateau (for F-Benz) at ≈7.0 and 7.7 Å, respectively. The first shell is ill-defined but somewhat more extended with the bigger solute. There is also extensive exchange between this shell and the "bulk" solvent CO_2 molecules. The average lifetime of one CO_2 molecule in the first shell of both solutes is ≈5 ps. Integration of the first peak gives a higher coordination number (CN) for F-Benz than for H-Benz (18 ± 2 *vs.* 13 ± 2, respectively, at 305 or 350 K) and a higher CN for F-Tol than for H-Tol (21 ± 1 *vs.* 14 ± 2), thus leading to larger interactions with the fluorinated compounds. Looking now at the solvation contribution of the first-shell CO_2 molecules (Table 3), one sees that with the four studied solutes they contribute 95% or more of the total interaction energy ΔE, as expected from the short range character of van der Waals interactions.

X-Aryls at the CO_2–water interface

The benzene derivatives are hydrophobic and we wanted to compare their behavior at a CO_2–water interface. During the dynamics, they remain on the CO_2 side of the interface and none moved to the aqueous phase, as expected. Their distance from the interface is plotted in Fig. 8. Comparison of H-Benz with F-Benz reveals interesting effects of fluorination and temperature. During the dynamics at 305 K, the H-Benz molecule always remains close to the interface (at 2.3 ± 2.7 Å, on average) and oscillates a few Ångströms apart. It is thus somewhat surface-active and the reason can be found in specific OH–π interactions between interfacial water molecules and the aromatic ring, as found in the gas phase[30] or in condensed phases.[31,32] This contrasts with the F-Benz molecule, which diffuses into the CO_2 phase from one interface to the other, and comes back to the initial one in less than 0.5 ns. It sits, on average, in the center of the CO_2 phase, at 14 ± 8 Å from the interface. F-Benz is thus not surface-active and is more soluble than H-Benz in bulk CO_2, in keeping with the above results in CO_2 solution. Its lifetime near the interface is short (< 10 ps) but a snapshot reveals interesting differences, compared to H-Benz (Fig. 9). Both solutes sit roughly parallel to the interface, hydrated on one face and solvated by CO_2 on the other face. The nearest CO_2 molecules are parallel to the ring of H-Benz and rather "perpendicular" to the ring of F-Benz. Water does not make OH–π interactions with F-Benz, but sits rather tangential to the ring and exhibits very labile CF···HO interactions. At 350 K, the F-Benz molecule again sits in the CO_2 phase with short excursions to the interface(s), while H-Benz remains close to the starting interface (at 5.9 ± 6.2 Å, on average). Its lifetime at the interface thus decreases at higher temperature, but is still represents ≈50% of the total simulated time. We notice that the surface activity of benzene is consistent with experimental results at the water–air interface, which bears some analogies with the CO_2–water interface.[33] Another analogy concerns halogenated alkanes whose free energy profiles display a minimum at the water–hexane interface.[34]

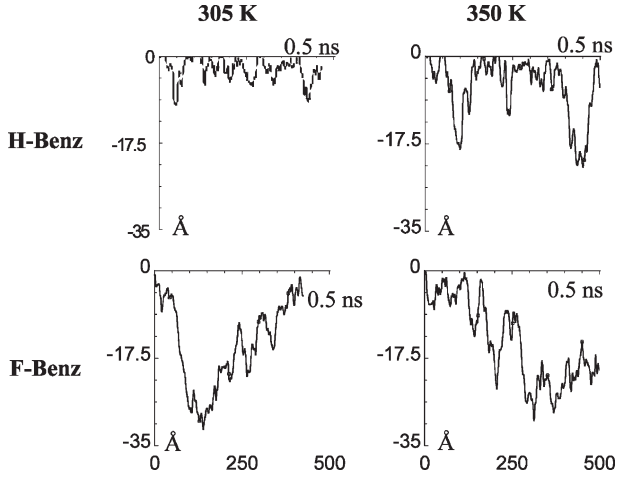

Fig. 8 H-Benz and F-Benz at a CO_2–water interface: distances from the interface (Å) at a function of time (ps) at 305 and 350 K.

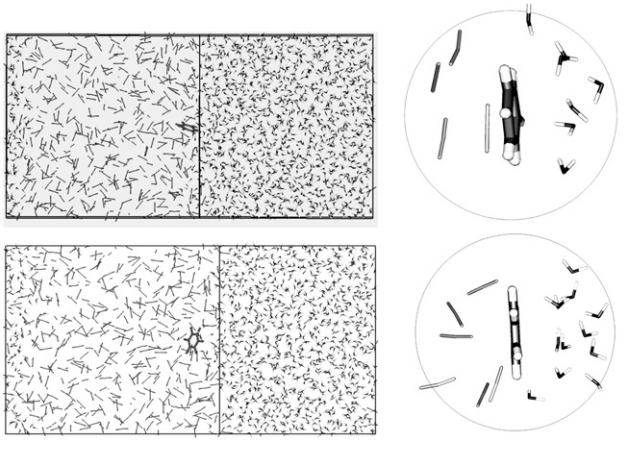

Fig. 9 H-Benz (top) and F-Benz (bottom) at the CO_2–water interface at 305 K. Final views of the simulation box and first solvation shell of X-Benz.

Table 5 X-Aryls at the SC-CO_2–water interface. Average interaction energies (kcal mol^{-1}) and their components at 305 nd 350 K.

		CO_2			H_2O		
Solute	T	Electr.	vdW	Total	Electr.	vdW	Total
H-Benz	305	-0.9 ± 0.8	-6.6 ± 1.8	-7.5 ± 2.3	-3.0 ± 2.7	-2.8 ± 1.4	-5.9 ± 3.3
F-Benz	305	-1.6 ± 0.8	-11.1 ± 1.6	-11.7 ± 1.7	-0.1 ± 0.2	-0.1 ± 0.5	-0.2 ± 0.5
H-Benz	350	-0.7 ± 0.8	-6.4 ± 2.0	-7.1 ± 2.0	-1.5 ± 1.6	-1.7 ± 1.7	-3.2 ± 2.4
F-Benz	350	-1.2 ± 0.9	-10.4 ± 2.0	-10.6 ± 2.2	-0.1 ± 0.6	-0.5 ± 0.6	-0.6 ± 0.1
H-Tol	350	-0.7 ± 0.7	-8.3 ± 1.0	-9.0 ± 2.1	-0.1 ± 1.6	-1.0 ± 1.4	-2.4 ± 2.7
F-Tol	350	-0.8 ± 0.5	-9.2 ± 1.6	-10.0 ± 1.8	-1.0 ± 0.9	-1.6 ± 1.4	-2.6 ± 2.3

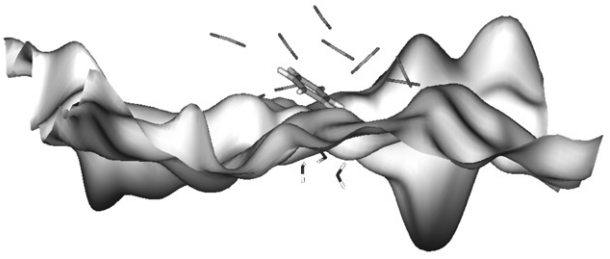

Fig. 10 H-Benz at a CO_2–water interface at 305 K. Water surface at the interface after 1 ns.

The analysis of average interaction energies (Table 5) confirms that H-Benz interacts better than F-Benz with the water phase (-5.9 *vs.* -0.2 kcal mol^{-1}, respectively), while F-Benz interacts better than H-Benz with the CO_2 phase (-11.7 *vs.* -7.5 kcal mol^{-1}, respectively, at 305 K). Decomposition into van der Waals and electrostatic components shows that the former accounts for more than 90% with CO_2 and about 50% with water. When the temperature increases to 350 K, interactions with both phases are somewhat weaker, as expected (Table 5). Fig. 10 shows the instant surface of water at the interface, with the adsorbed H-Benz molecule. The interface is instantaneously quite rough, about 14 Å thick and highly mobile, as found in other studies.[14,35]

Conclusions

We have presented theoretical investigations on the effect of fluorination of simple aromatic compounds in a SC-CO_2 solution, as well as in small clusters with CO_2. Despite the low polarity of the CO_2 molecule, specific solvation patterns are observed, depending on the H *vs.* F substituents. In small clusters, CO_2 interactions with fluorinated solutes are weaker than with hydrogenated ones and involve different types of facial complexes. However, with more than 6 CO_2 molecules, the order inverts and F compounds are better solvated. We note that H-Benz$(CO_2)_n$ clusters have been characterized experimentally with $n = 1$ to 6, while larger ones do not seem to be stable.[27] The CO_2-philic character of fluorinated compounds is also confirmed by free energy perturbation calculations in SC-CO_2 solution, which also hint at more pronounced differentiation at lower temperatures. Another facet of fluorination emerges from simulations at the CO_2–water interface, where benzene somewhat adsorbs, while its perfluorinated analog does not and solubilizes therefore more in the CO_2 phase. We notice that fluorinated amphiphilic compounds generally have a lower CMC (critical micellar concentration) than their hydrogenated analogs and are more surface-active.[36,37] Our results concern small non-amphiphilic solutes whose interactions with solvents are weak. The "stereochemistry" (preferred orientation) of first-shell molecules in the SC-CO_2 solution and of water molecules at the interface is determined by electrostatic interactions (of the quadrupole-quadrupole and quadrupole-dipole type, respectively), but overall the energetics is dominated by the cumulated van der Waals contacts, which increase upon H → F substitution, that is with the surface of the solute. Although these contributions may be method- and model-dependent (see, *e.g.*, issues with the Lorentz–Berthelot mixing rules)[38,39] we feel that the analysis based on simple force field approaches gives valuable insights into the CO_2-philicity of fluorinated compounds. Similar force field approaches have been used to study, for example, the solubility of xenon or oxygen in alkanes *vs.* perfluoroalkanes,[40,41] benzene[28,42] or aromatic compounds[43] in SC-CO_2. Comparison at different temperatures also reveals the importance of dynamics. The decrease in interactions when the systems is heated is certainly much larger than "inaccuracies" in the representation of the potential energy.

Acknowledgements

The authors are grateful to IDRIS, CINES and Université Louis Pasteur for computer resources. E. Engler is acknowledged for software developments. NG thanks the French Ministry of Research for a grant. .WG thanks Professor A. Dedieu for stimulating discussions.

References

1 K. E. Laintz, C. M. Wai, C. R. Yonker and R. D. Smith, *J. Supercrit. Fluids*, 1991, **4**, 194.
2 T. A. Hoefling, R. M. Enick and E. J. Bechman, *J. Phys. Chem.*, 1991, **95**, 7127.
3 A. Laitinen, O. Jauhiainen and O. Aaltonen, *Org. Process Res. Dev.*, 2000, **4**, 353.
4 M. P. Krafft and J. C. Riess, *Biochimie*, 1998, **80**, 489.
5 R. Enick, E. Beckman, A. Yazdi, V. Krukonis, H. Schonemann and J. Howell, *J. Supercrit. Fluids*, 1998, **13**, 121.
6 P. Raveendran and S. L. Wallen, *J. Phys. Chem. B*, 2003, **107**, 1473.
7 J. E. Brady and P. W. Carr, *J. Phys. Chem.*, 1985, **89**, 1813.
8 G. G. Yee, J. L. Fulton and R. D. Smith, *J. Phys. Chem.*, 1992, **96**, 6172.
9 C. R. Yonker, *J. Phys. Chem. A*, 2000, **104**, 685.
10 A. Dardin, J. M. De Simone and E. T. Samulski, *J. Phys. Chem. B*, 1998, **102**, 1775.
11 A. Cece, S. H. Jureller, J. L. Kerscher and K. F. Moschner, *J. Phys. Chem. A*, 1996, **100**, 7435.
12 P. Diep, K. D. Jordan, J. K. Johnson and E. J. Beckman, *J. Phys. Chem. A*, 1998, **102**, 2231.
13 Y.-K. Han and H. Y. Jeong, *J. Phys. Chem. A*, 1997, **101**, 5604.
14 R. Schurhammer, F. Berny and G. Wipff, *Phys. Chem. Chem. Phys.*, 2001, **3**, 647; R. Schurhammer and G. Wipff, *New J. Chem.*, 2021, **26**, 229; M. Baaden, R. Schurhammer, F. Berny and G. Wipff, *J. Phys. Chem. B*, 2002, **106**, 434; P. Vayssière and G. Wipff, *Phys. Chem. Chem. Phys.*, 2003, **5**, 127; P. Vayssière and G. Wipff, *Phys. Chem. Chem. Phys.*, 2003, **5**, 2842.
15 Y. Lin, R. D. Brauer, K. E. Laintz and C. M. Wai, *Anal. Chem.*, 1993, **65**, 2549.
16 N. G. Smart, T. Carleson, T. Kast, A. A. Clifford, M. D. Burford and C. M. Wai, *Talanta*, 1997, **44**, 137.
17 D. A. Case, D. A. Pearlman, J. C. Caldwell, T. E. Cheatham III, W. S. Ross, C. L. Simmerling, T. A. Darden, K. M. Merz, R. V.

Stanton, A. L. Cheng, J. J. Vincent, M. Crowley, D. M. Ferguson, R. J. Radmer, G. L. Seibel, U. C. Singh, P. K. Weiner, P. A. Kollman, AMBER5, University of California, San Francisco, 1997.
18 C. A. Gough, S. E. DeBolt and P. A. Kollman, *J. Comput. Chem.*, 1992, **13**, 963.
19 C. S. Murthy, K. Singer and I. R. McDonald, *Mol. Phys*, 1981, **44**, 135.
20 W. L. Jorgensen, J. Chandrasekhar, J. D. Madura, R. W. Impey and M. L. Klein, *J. Chem. Phys.*, 1983, **79**, 926.
21 I. G. Tironi, R. Sperb, P. E. Smith and W. F. van Gunsteren, *J. Chem. Phys.*, 1995, **102**, 5451.
22 M. Kettler, I. Nezbeda, A. A. Chialvo and P. T. Cummings, *J. Phys. Chem. B*, 2002, **106**, 7537.
23 B. F. Graham, A. F. Lagalante, T. J. Bruno, J. M. Harrowfield and R. D. Trengove, *Fluid Phase Equilib.*, 1998, **150–151**, 829.
24 G. Wipff, E. Engler, P. Guilbaud, M. Lauterbach, L. Troxler and A. Varnek, *New J. Chem.*, 1996, **20**, 403.
25 H. J. C. Berendsen, J. P. M. Postma, W. F. van Gunsteren and A. DiNola, *J. Chem. Phys.*, 1984, **81**, 3684.
26 P. Kollman, *Chem. Rev.*, 1993, **93**, 2395.
27 R. Nowak, J. A. Menapace and E. R. Bernstein, *J. Chem. Phys.*, 1988, **89**, 1309.
28 J. W. Shen, O. Kitao and K. Nakanishi, *Fluid Phase Equilib.*, 1996, **120**, 81.
29 R. A. Pierotti, *Chem. Rev.*, 1976, **76**, 717.
30 M. Raimondi, G. Calderoni, A. Famulari, L. Raimondi and F. Cossi, *J. Phys. Chem. A*, 2003, **107**, 772.
31 E. A. Meyer, R. K. Castellano and F. Diederich, *Angew. Chem., Int. Ed.*, 2003, **42**, 1210.
32 T. Steiner and G. Koellner, *J. Mol. Biol.*, 2001, **305**, 535.
33 J. R. G. Bruant and M. H. Conklin, *J. Phys. Chem. B*, 2002, **106**, 2232.
34 C. Chipot, M. A. Wilson and A. Pohorille, *J. Phys. Chem. B*, 1997, **101**, 782.
35 S. R. P. D. Rocha and K. P. Johnston, *Langmuir*, 2000, **16**, 3690.
36 E. Kissa, *Fluorinated Surfactants. Synthesis. Properties. Applications*, M. Dekker, New York, 1994.
37 V. M. Sadtler, F. Giulieri, M.-P. Krafft and J. G. Riess, *Chem.-Eur. J.*, 1998, **4**, 1952.
38 T. A. Halgren, *J. Am. Chem. Soc.*, 1992, **114**, 7827.
39 A. Varnek, S. Helissen, G. Wipff and A. Collet, *J. Comput. Chem.*, 1998, **19**, 820.
40 R. P. Bonifacio, C. McCabe, E. Filipe, M. F. C. Gomes and A. A. H. Padua, *Mol. Phys.*, 2002, **5**, 2547.
41 A. M. A. Dias, R. P. Bonifacio, I. M. Marrucho, A. A. H. Padua and M. F. C. Gomes, *Phys. Chem. Chem. Phys.*, 2003, **5**, 543.
42 H. Inomata, S. Saito and P. G. Debenedetti, *Fluid Phase Equilib.*, 1996, **116**, 282.
43 L. A. F. Coelho, A. Marchut, J. V. de Oliveira and P. B. Balbuena, *Ind. Eng. Chem. Res.*, 2000, **39**, 227.